Journal of Alloys and Compounds 501 (2010) 255–258

Contents lists available at ScienceDirect

Journal of Alloys and Compounds

journal homepage: www.elsevier.com/locate/jallcom

Lithium storage capability of lithium ion conductor $Li_{1.5}Al_{0.5}Ge_{1.5}(PO_4)_3$

J.K. Feng, L. Lu*, M.O. Lai

Department of Mechanical Engineering, National University of Singapore, 9, Engineering Drive 1, Singapore

ARTICLE INFO

Article history:
Received 2 February 2010
Received in revised form 12 April 2010
Accepted 14 April 2010
Available online 22 April 2010

Keywords:
Solid-state electrolyte
Lithium battery
Anode

ABSTRACT

$Li_{1.5}Al_{0.5}Ge_{1.5}(PO_4)_3$ (LAGP) with a NASICON ($LiM_2(PO_4)_3$) structure has been successfully prepared using solid-state reaction. Structural characterization shows $LiM_2(PO_4)_3$ to be the main phase. The total conductivity of the as-prepared LAGP is about 3.5×10^{-6} S/cm with an electrical conductivity of 10^{-9} S/cm. Electrochemical study reveals that the LAGP is stable up to 7 V with a slight reduction at about 0.85 V (vs. Li/Li^+). For the first time, the electrochemical performance of the LAGP as an anode for lithium battery is tested, showing that the LAGP could be used as an anode material with good cycleability.

1. Introduction

All-solid-state lithium ion batteries are promising power sources for large scale applications because of their high safety, excellent cycleability and low packing cost compared to common batteries using liquid electrolyte. Among all components in the all-solid-state lithium ion batteries, the solid electrolyte is one of the most important key components that controls the properties of the batteries. The solid electrolytes must meet a number of requirements before they can be practically used, including high conductivity, large cationic transport number, wide potential window and low electronic conductivity [1–4].

In the past decades, extensive investigations have been carried out on NASICON-type structured lithium ion conductor with the general formula of $LiM_2(PO_4)_3$ where M is the tetravalent cation that possesses high ionic conductivity. $LiTi_2(PO_4)_3$ based materials with NASICON-type structure have the most suitable tunnel size for Li ion migration among the series of $Li_{1+x}A_xM_{2-x}(PO_4)_3$ (M = Ti, Ge, Hf, Sr, Zr, Sn, etc. and A = Al, La, In, Cr, etc.) [5–20]. However, since they consist of Ti^{4+} ions, they are easy to be reduced when they are in contact with lithium metal, hence limiting their applications [5–12].

Recently, the glass-ceramic $Li_{1+x}Al_xGe_{2-x}(PO_4)_3$ (LAGP) has gained special interest because it is particularly stable against Li metal and has a high ionic conductivity (as high as 4.62×10^{-3} S/cm at 27 °C) [16,21–27]. Partial substitution of Ge^{4+} with Al^{3+} has shown improved porous density of $LiGe_2(PO_4)_3$ as well as enhanced Li^+ ion conductivity. It has also been found that Ge and Ge oxide are capable of interaction with lithium to form Li_xGe alloy compounds [28–30], which means that Ge compounds are capable of electrochemical reactive at low voltage. Therefore it would be interested to know whether LAGP is electrochemically stable with lithium.

In the present work, Ge instead of GeO_2 has been used to synthesize $Li_{1.5}Al_{0.5}Ge_{1.5}(PO_4)_3$ through solid-state process at a low temperature. The electrochemical properties of the LAGP have been systematically investigated by means of cyclic voltammetry, AC impedance, DC conductivity measurement and battery test.

2. Experimental

Stoichiometric amounts of lithium carbonate (Aldrich), aluminum oxide (Aldrich), germanium (Aldrich), and ammonium dihydrogen phosphate (Aldrich) were used as the starting materials to prepare LAGP by a conventional solid solution method. 10% excess lithium carbonate was employed to compensate loss of lithium during the processing. The powder mixture was first thoroughly mixed by ball milling and then heated in a platinum crucible at 700 °C for 2 h to release any volatile compounds. The synthesized powders were then reground followed by calcination at 950 °C under a heating rate of 1 °C/min for 2 h. The as-prepared product was cold-compacted into pellets at 10 MPa for 20 min and then sintered at 950 °C for 10 h.

Structure of the synthesized powders was investigated using a Shimadzu XRD-6000 X-ray diffractometer with Cu Ka radiation. The data were collected at a scan rate of 2°/min. Surface morphology of the sintered pellets was characterized using a Hitachi S-4100 field emission scanning electron microscopy.

AC impedance and steady-state DC electronic current measurements were carried out using a Solartron impedance analyzer (model 1260) in the frequency range between 10^{-1} Hz and 10^6 Hz [2]. To study the electrical and ionic behaviors of the specimens, Ag was coated onto one or two sides of the specimens according to whether lithium reference and counter electrode were needed. The Ag-coated specimen was assembled into a cell using stainless steel (SS) as current collector to test the AC impedance [22]. To study the cyclic voltammetric (CV) performance of the specimens, one side of the specimen was coated with a Ag layer as a working electrode while the other side was attached with a lithium foil as a counter electrode.

Steady-state DC electronic current measurements and CV were undertaken to obtain the electronic conductivity and electrochemical window of the electrolyte

* Corresponding author. Fax: +65 67791459.
E-mail addresses: luli@nus.edu.sg, mpeluli@nus.edu.sg (L. Lu).

0925-8388/$ – see front matter © 2010 Elsevier B.V. All rights reserved.
doi:10.1016/j.jallcom.2010.04.084

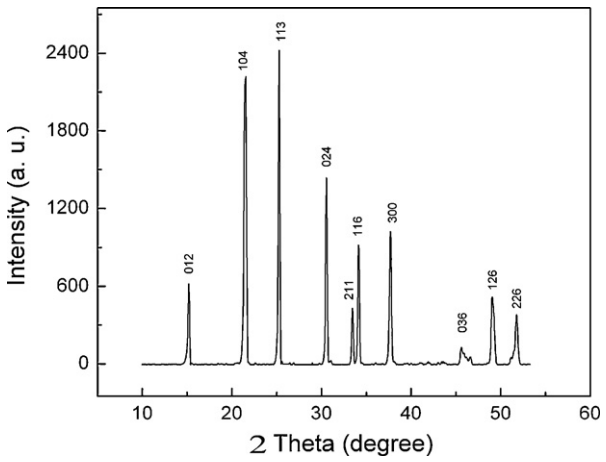

Fig. 1. X-ray diffraction spectrum of the LAGP sintered at 950 °C for 10 h.

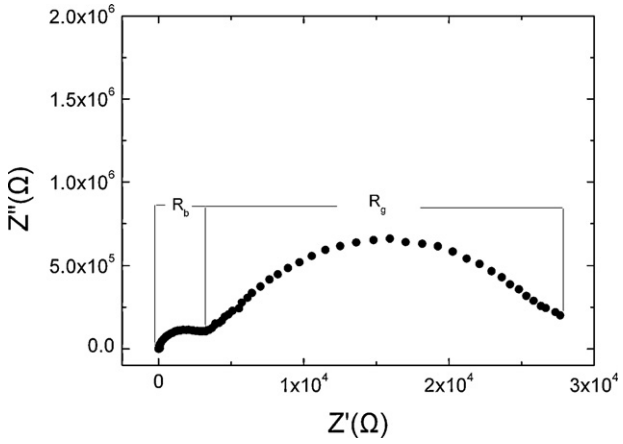

Fig. 3. Complex impedance plot for LAGP pellet at room temperature.

using an electrochemical work station (Solartron 1287) with a scanning rate of 0.1 mV/s between −0.6 V and 7 V [2].

Battery test was carried out using a Solartron 1287 two terminal cell test system with a laboratory-made cell. The working electrode consisted of 80% LAGP, 10% acetylene black and 10% PTFE binder as working electrode. A lithium foil was used as both counter and reference electrodes. 1 M $LiPF_6$ in ethyl carbonate/dimethyl carbonate solution (EC/DEC, 1/1 vol% Ozark Fluorine Specialties, Inc.) was used as the electrolyte. Galvanostatic charge/discharge cycling experiment was performed in the potential range from 0.01 V to 2.5 V at a current density of 0.1 mA/cm^2.

3. Results and discussion

Fig. 1 shows the XRD pattern of the $Li_{1.5}Al_{0.5}Ge_{1.5}(PO_4)_3$ calcined at 950 °C for 24 h. All the diffraction peaks of the specimen are well matched with NASICON $LiGe_2(PO_4)_3$ (JCPDS 41-0034) structure [16,21–27], indicating that LAGP has been formed. Although 25% of Ge has been substituted by Al, the diffraction peaks are not dramatically shifted, attributing to the similarity in ionic radius between Ge^{4+} (0.053 nm) and Al^{3+} (0.050 nm).

The scanning electron microcopy (SEM) image of the specimen is shown in Fig. 2. It can be seen that the LAGP sample consists of large crystallized grains (particles) of about 2 μm together with featureless image which may be amorphous phase. It is known that electrical conductivity consists of two contributions from grain and grains boundaries. The reduction in grain boundaries by increasing the grain size and incorporating with low boundary glass electrolyte may greatly reduce the grain boundary resistance [24,25].

A typical AC impedance spectrum of the LAGP sample is shown in Fig. 3. Two semicircles are observed. The semicircle in the high frequency range is due to the bulk ionic resistance while the appearance of the low-frequency semicircle is an indication of the grain boundary resistance of NASICON-type material [16,24,25]. The grain boundary resistance is relatively large due to the well crystallization. The total resistance, R_t, of the samples can be approximately obtained from the right intercept of the second semicircle with the real axis in the plot while the bulk resistance, R_b, may be obtained from the left intercept of the first semicircle with the real axis. From Fig. 3, the total conductivity, σ, is evaluated to be 3.5×10^{-6} S/cm from $\sigma = d/(R_t A)$ where d (0.2 cm) is the thickness of the sample and A (2 cm^2) is the surface area of the pellet. The conductivity of the sample, although comparable with most reported data [16,22–24], is lower than the best data reported [25].

Fig. 4 shows the electrical conductivity of LAGP measured by DC polarization using Ag/LAGP/Li electrode between 0 V and 7 V (vs. Li/Li^+). The steady-state current is caused only by the flow of electrons and holes. The estimated electrical conductivity is about 10^{-9} S/cm at room temperature. However, a sharp increase of about 10 times in electrical conductivity is observed at below 0.85 V. The increase in electrical conductivity is due mainly to the reduction of the sample. Although there is a large increase in electrical conductivity, its final value is still low (10^{-7} S/cm). The LAGP sample is therefore still acceptable for application as electrolyte. The transference number of lithium is calculated to

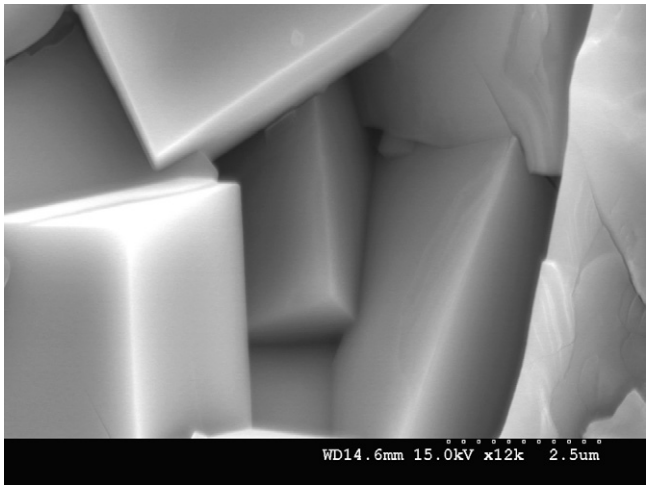

Fig. 2. SEM micrograph of fracture surface of sintered LAGP.

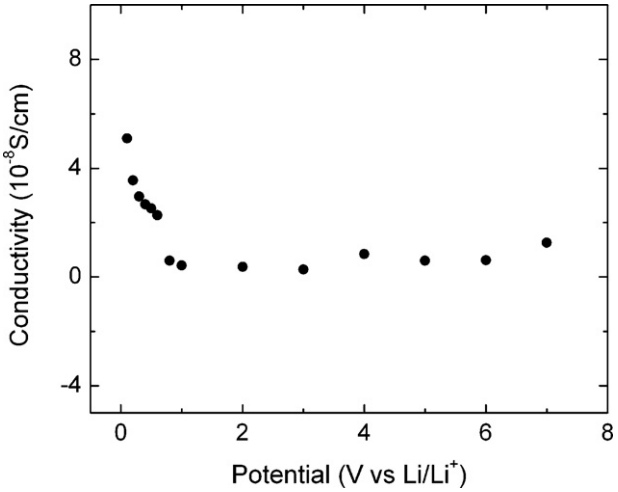

Fig. 4. Steady-state electronic conductivity vs. potential of SS/LAGP/Li.

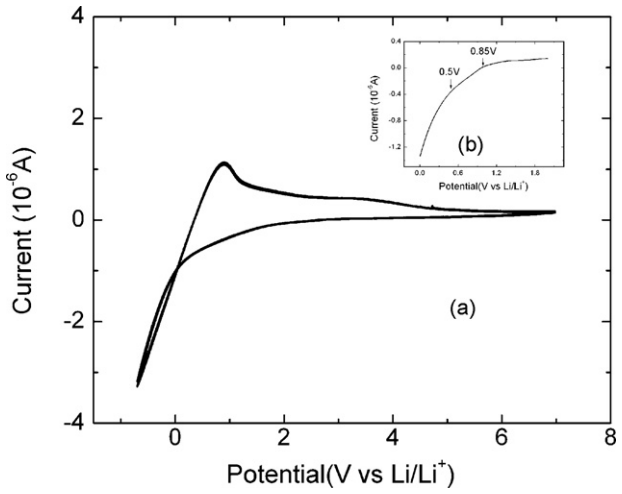

Fig. 5. (a) Cyclic voltammogram of Ag/LAGP/Li recorded at a scanning rate of 0.1 mV/s and (b) CV curve of LAGP between 0 V and 1 V (vs. Li/Li$^+$).

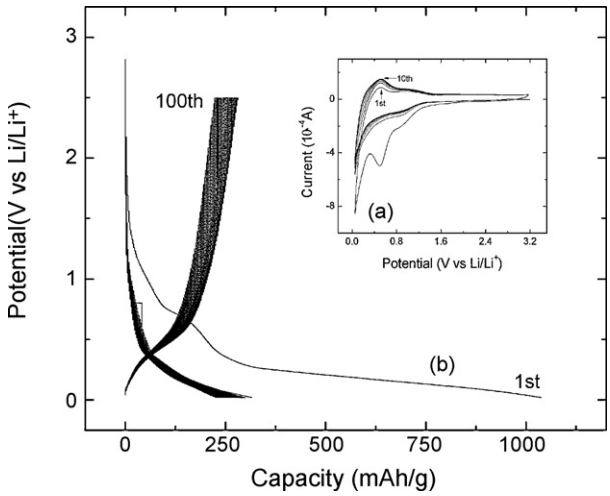

Fig. 6. (a) The 10th CV curves and (b) the 1st–100th charge–discharge profiles of LAGP/liquid electrolyte/Li half cell.

be nearly unity ($t_{Li+} = (\sigma_{total} - \sigma_{electronic})/\sigma_{total} \approx 1$), where the conductivity ($\sigma_{ionic} = 3.5 \times 10^{-6}$ S/cm) is taken from the AC impedance measurement).

Fig. 5(a) shows the CV for the LAGP/Li at a scanning rate of 0.1 mV/s. Reduction current is observed from 0.8 V (vs. Li/Li$^+$) indicating a slight reduction of the LAGP at low voltage. Between −0.8 V and 0.8 V there is a pair of reversible peaks corresponding to the deposition and dissolution of lithium [3], implying that the LAGP is capable of reduction at very low potential without affecting the lithium conducting property of the LAGP. No other peaks are observed in the potential range up to 7 V (vs. Li/Li), indicating an at least 6.2 V of electrochemical window for the LAGP.

The reactions of the LAGP with lithium at low potential (0–1 V vs. Li/Li$^+$) are shown in Fig. 5(b). From the figure, a clear reduction current can be seen to arise at 0.85 V (vs. Li/Li$^+$) clearly due to the reduction of LAGP, which may indicate that the LAGP start to reduction at 0.85 V (vs. Li/Li$^+$), causing the change in electronic conductivity [12–15].

As LAGP can react with lithium, it may be used as an active material as the anode of lithium battery. To examine the battery performance of the LAGP composite anode, CV and 100 charge/discharge cycles were carried out. Fig. 6(a) shows the first 10 CV plots of LAGP/LiPF$_6$ EC + DMC/Li cell. It can be seen that there are three reduction peaks at 1.0 V, 0.8 V and 0.4 V, respectively, which correspond to the reduction of LAGP, solid electrolyte interface (SEI) formation and Li$_x$Ge formation [28–30]. An oxidation peak due to lithium de-intercation appears when scanned at the positive direction. From the second cycle, only the peaks of lithium alloy and de-alloy with Ge can be observed. There is only minor change in the peak area after 10 cycles, illustrating that the alloying and de-alloying progress is almost completely reversible. Fig. 6(b) shows the charge/discharge curves for 100 cycles between 0 V and 2.5 V at a current density of 0.1 mA/cm^2 corresponding to a rate of 150 mA/g. For the first discharge process, a plateau at 0.8 V due to the reduction of electrolyte can be observed. The voltage of the cell then decreases from 0.5 V and slowly down to 0 V. This is similar to the first charge–discharge curve of GeO_2 compounds [30]. The first discharge capacity is 1100 mAh/g, while the first charge capacity is about 340 mAh/g. The efficiency of the first cycle is about 30.9%, lower than the ideal efficiency of 52% ($Li_{4.4}Ge/2Li_2O + Li_{4.4}Ge$). The relatively low efficiency is probably caused by the formation of SEI film on conductive carbon black. From the second curve, only charge and discharge curves between 0.01 V and 0.5 V are seen, which is similar to the Ge alloying and de-alloying with lithium [28,29]. The mechanism is assumed to be as follows:

$$Li_{1.5}Al_{0.5}Ge_{1.5}(PO_4)_3 + 6Li^+ + 6e^- \rightarrow 1.5Ge + 2.5Li_3PO_4 + 0.5AlPO_4 \quad (1)$$

and

$$1.5Ge + 6.6Li^+ + 6.6e^- \rightarrow 1.5Li_{4.4}Ge \quad (2)$$

It can be seen from Fig. 6(a) that the voltage profiles of subsequent charge/discharge cycles show only a slight difference between the 1st charge curve and the 100th curve. A reversible capacity of about 300 mAh/cm with good retention and almost 100% column efficiency after the first charge/discharge is obtained. This capacity is acceptable compared to the ideal capacity of LAGP (410 mAh/g calculated from $Li_{4.4}Ge$). As reported before, the cycling performance of bulk GeO_2 as an anode is relatively poor due to the large volume change during cycling (drops from 740 mAh/g to 225 mAh/g after 10 cycles) [30]. The reason for the poor cycleability is the volume change during charge and discharge, leading to disconnection between active material and current collector, and aggregation of active element as shown by Dahn et al. [31,32]. The excellent capacity retention in the present study may be due to the formation of the by-products Li_3PO_4 and $AlPO_4$, which form an inactive matrix that buffers the change in volume during the alloy and de-alloy process, hence inhabiting the aggregation of Ge. The mechanism is illustrated in Fig. 7. The LAGP is first reduced to little Ge particles surrounded by Li_3PO_4 and $AlPO_4$. Then Ge alloys and de-alloys with lithium. Since Ge is surrounded by Li_3PO_4 and

Fig. 7. Possible mechanism of LAGP used as lithium anode material.

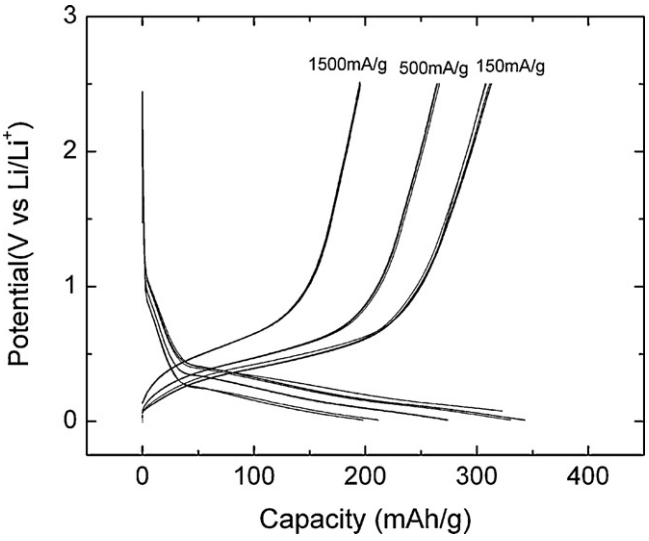

Fig. 8. Rate capability of LAGP/liquid electrolyte/Li half cell at different charge–discharge rates.

$AlPO_4$, the surroundings buffer the change in volume during the charge and discharge. Moreover, Li_3PO_4 can provide a Li conducting channel for Li ion diffusion [33].

The rate capability of the LAGP anode at different rates is also studied. Fig. 8 shows the variation of capacities of the LAGP at different rates. The capacity of the LAGP at the rate of 1500 mA/g maintains about 60% of the capacity at the rate of 150 mA/g. The good rate capability may be due to the relatively high lithium conductivity of the by-product Li_3PO_4 which surrounds the active Ge compound, leading to an enhanced lithium ion transfer rate [8,33,34].

4. Conclusions

NASICON-type structured ceramic $Li_{1.5}Al_{0.5}Ge_{1.5}(PO_4)_3$ has been successfully prepared at a low temperature. Structural analysis revealed $LiGe_2(PO_4)_3$ to be the main phase. The ionic conductivity is about 3.5×10^{-6} S/cm and the electronic conductivity is in the order of 10^{-9} S/cm. Electrochemical analysis showed that the LAGP was stable up to 7 V while a slight reduction appeared at 0.85 V. For the first time, the battery performance of the LAGP has been measured. Results showed that LAGP could be used as an anode material for lithium battery with good cycleability.

Acknowledgement

The authors wish to acknowledge the Agency for Science, Technology and Research of Singapore (A-Star) for the financial support through a research grant R-265-000-292-731 (072 134 0051).

References

[1] Y. Kobayashi, S. Seki, A. Yamanaka, H. Miyashiro, Y. Mita, T. Iwahori, J. Power Sources 146 (2005) 719–722.
[2] J. Schwenzel, V. Thangadurai, W. Weppner, J. Power Sources 154 (2006) 232–238.
[3] N.J. Dudney, Mater. Sci. Eng. B 116 (2005) 245–249.
[4] H.X. Geng, A. Mei, C. Dong, Y.H. Lin, C.W. Nan, J. Alloys Compd. 481 (2009) 555–558.
[5] T. Jiang, Y.J. Wei, W.C. Pan, Z. Li, X. Ming, G. Chen, C.Z. Wang, J. Alloys Compd. 488 (2009) L26–L29.
[6] K. Takada, M. Tansho, I. Yanase, Y. Inada, A. KajiyaMa, M. Konguchi, S. Kondo, M. Watanade, Solid State Ionics 139 (2001) 241–247.
[7] K.Y. Yang, J.W. Wang, K.Z. Fung, J. Alloys Compd. 458 (2009) 415–424.
[8] J.K. Feng, H. Xia, M.O. Lai, J. Phys. Chem. C 113 (2009) 20514–20520.
[9] G. Govindaraj, C.R. Mariappan, Solid State Ionics 147 (2002) 49–59.
[11] Q.X. Zhang, Z.Y. Wen, Y. Liu, J. Alloys Compd. 479 (2009) 494–499.
[12] N. Anantharamulu, K.K. Rao, M. Vithal, G. Prasad, J. Alloys Compd. 479 (2009) 684–691.
[13] J. Fu, Solid State Ionics 96 (1997) 195–200.
[14] X. Li, M.Z. Qu, Z.L. Yu, J. Alloys Compd. 487 (2009) L12–L17.
[15] S.Q. Liu, S.C. Li, K.L. Huang, B.L. Gong, G. Zhang, J. Alloys Compd. 450 (2008) 499–504.
[16] X.L. Yao, S. Xie, H.Q. Nian, C.H. Chen, J. Alloys Compd. 465 (2008) 375–379.
[17] C.Q. Zhang, J.P. Tu, X.H. Huang, Y.F. Yuan, S.F. Wang, F. Mao, J. Alloys Compd. 457 (2008) 81–85.
[18] J.S. Thokchom, B. Kumar, J. Power Sources 185 (2008) 480–485.
[19] K. Arbi, J.M. Rojo, J. Sanz, J. Eur. Ceram. Soc. 27 (2007) 4215–4218.
[20] E. Kazakevičius, A. Určinskas, A. Kežionis, A. Dindune, Z. Kanepe, J. Ronis, Electrochim. Acta 27 (2006) 6199–6202.
[21] B.V.R. Chowdari, G.V. Subba Rao, G.Y.H. Lee, Solid State Ionics 136–137 (2000) 1067–1075.
[22] E. Kazakevičius, T. Šalkus, A. Dindune, Z. Kanepe, J. Ronis, A. Kežionis, V. Kazlauskienė, J. Miškinis, A. Selskienė, A. Selskis, Solid State Ionics 179 (2008) 51–56.
[23] M. Cretin, P. Fabry, J. Eur. Ceram. Soc. 19 (1999) 2931–2940.
[24] X.X. Xu, Z.Y. Wen, X.W. Wu, X.L. Yang, Z.H. Gu, J. Am. Ceram. Soc. 90 (2007) 2802–2806.
[25] J.S. Thokchom, N. Gupta, B. Kumar, J. Electrochem. Soc. 155 (2008) A915–A920.
[26] C.J. Leo, B.V.R. Chowdari, G.V. Subha Rao, J.L. Souquet, Mater. Res. Bull. 37 (2002) 1419–1430.
[27] S. Rani, S. Sanghi, A. Agarwal, N. Ahlawat, J. Alloys Compd. 477 (2009) 504–509.
[28] C.K. Chan, X.F. Zhang, Y. Cui, Nano Lett. 8 (2008) 307–309.
[29] H. Lee, M. Gyu Kim, C.H. Choi, Y.K. Sun, C.S. Yoon, J. Cho, J. Phys. Chem. B 109 (2005) 20719–20723.
[30] J.S. Pena, I. Sandu, O. Joubert, F.S. Pascual, C.O. Arean, T. Brousseb, Electrochem. Solid-State Lett. 9 (2004) A278–A281.
[31] I.A. Courtney, J.R. Dahn, J. Electrochem. Soc. 144 (1997) 2943–2948.
[32] M.G. Kim, J. Cho, J. Electrochem. Soc. 156 (2009) A277–A282.
[33] B. Kang, G. Ceder, Nature 458 (2009) 190–193.
[34] S.Q. Zhang, S. Xie, C.H. Chen, Mater. Sci. Eng. B 121 (2005) 160–165.